Vectorial release of matrix metalloproteinases (MMPs) from porcine RPE-choroid explants following selective retina therapy (SRT): Towards slowing the macular ageing process

F. Treumer [a,*], A. Klettner [a], J. Baltz [a], A.A. Hussain [b], Y. Miura [c], R. Brinkmann [c], J. Roider [a], J. Hillenkamp [a]

[a] Department of Ophthalmology, University Medical Center Schleswig-Holstein, Kiel, Germany
[b] Division of Molecular Therapy, UCL Institute of Ophthalmology, University of London, UK
[c] Institute of Biomedical Optics, University of Luebeck, Germany

ABSTRACT

The purpose of this study was to investigate release of matrix metalloproteinases (MMP) 2 and 9 during retinal pigment epithelium (RPE) wound healing after Selective Retina Therapy (SRT) with laser energy levels below and above the threshold of RPE cell death. Following exposure to SRT using a prototype pulsed Nd:YLF laser with energies of 80–180 mJ/cm^2 fresh porcine RPE-monolayers with Bruch's membrane and choroid were cultured in modified Ussing chambers which separate the apical (RPE-facing) and basal (choroid facing) sides of the RPE monolayer. Threshold energy for RPE cell death and wound healing were determined with calcein-AM viability test. Inactive and active forms of MMP 2 and 9 were quantified within tissue samples and in the culture medium of the apical and basal compartments of the Ussing chamber using gelatine zymography. Laser energies of 160–180 mJ/cm^2 resulted in cell death within 1 h while 120–140 mJ/cm^2 resulted in delayed death of exposed RPE cells. All cells survived 80 and 100 mJ/cm^2. Laser spots healed within 6 days after SRT accompanied by a transient vectorial increase of MMPs. SRT with 180 mJ/cm^2 increased active MMP 2 by 1.9 ($p < 0.05$) and 1.6 ($p < 0.05$) fold in tissue and basal compartments, respectively, without alterations in the apical compartment. Pro-MMP 2 levels were also significantly increased in all compartments ($p < 0.05$). Release of MMP 9 was not altered. Laser energy below the threshold of RPE cell death did not alter the release of MMP 2 or 9. The findings suggest that the release of active MMP 2 on the basal side of the RPE during wound healing following SRT may address age-related pathological changes of Bruch's membrane with a potential to slow degenerative macular ageing processes before irreversible functional loss has occurred.

© 2012 Elsevier Ltd. All rights reserved.

1. Introduction

Bruch's membrane (BrM) and the retinal pigment epithelium (RPE) mediate the bi-directional transport of nutrients and waste products between the photoreceptors of the retina and the choroidal blood supply. The matrix of BrM is continuously renewed by processes of coupled synthesis and degradation, the latter pathway being mediated by a family of proteolytic enzymes called the matrix metalloproteinases (MMPs) together with their inhibitors, TIMPs. The secretion of MMPs 1, 2, 3 & 9 and TIMPs 1, 2 & 3 by RPE and choroidal endothelial cells and their presence in BrM has been demonstrated (Alexander et al., 1990; Della et al., 1996; Fariss et al., 1997; Guo et al., 1999; Hunt et al., 1993; Vranka et al., 1997). TIMP-3 has been shown to be an integral component of BrM (Kamei and Hollyfield, 1999). Additional high molecular weight MMP species (termed HMW1&2) consisting of polymers of MMPs 2&9 and a much larger macromolecular weight complex (LMMC) comprising primarily of HMW 1, HMW 2, pro-MMP 9 together with some pro-MMP 2 have also been identified in human BrM (Hussain et al., 2010a; Kumar et al., 2010).

Despite the presence of this rejuvenation mechanism, ageing BrM shows gross functional and structural deterioration. The

capacity for transport of fluids, amino acids and larger molecular complexes, typified by carriers of metals, vitamins and lipids is severely curtailed (Hillenkamp et al., 2004a, 2004b; Hussain et al., 2010b; Moore et al., 1995; Moore and Clover, 2001; Starita et al., 1996). Reduced transport capability also implies impaired removal of membraneous debris extruded by the RPE and thus a vicious cycle is started with a potential to undermine the normal homeostatic support of the overlying photoreceptor layer.

Structural alterations of ageing BrM include increased thickness (Okubo et al., 1999; Ramrattan et al., 1994), the deposition of normal and abnormal extracellular matrix (ECM) material (Karwatowski et al., 1995), increased advanced glycation/lipoxidation end-products (AGEs and ALEs) (Handa et al., 1999) which are known to be potent inhibitors of MMP activity (Mott et al., 1997; Nagai et al., 2009; Yamada et al., 2006), the accumulation of lipid-rich debris (Holz et al., 1994; Pauleikhoff et al., 1992), and accumulation of inter-molecular fibril cross-links that have been shown to reduce the susceptibility of the collagen molecule to proteolytic action (Hamlin and Kohn, 1971; Vater et al., 1979). The age-related accumulation of high molecular weight MMP species has also been suggested to sequester monomeric species thereby removing them from the activation process (Hussain et al., 2010a). Thus levels of latent MMPs 2&9 were shown to increase with age but the presence of activated forms was scarce (Guo et al., 1999). All these changes suggest a disturbance in the turnover of the ECM of BrM.

The ageing changes observed in normal donors were much more exaggerated in BrM from donors with age-related macular degeneration (AMD). Hydraulic conductivity of BrM and diffusional capacity for amino acids and carrier sized molecules was severely compromised (Hillenkamp et al., 2004a; Hussain et al., 2010b; Moore and Clover, 2001; Moore et al., 1995; Starita et al., 1996). Abnormalities in the MMP system have been implicated as levels of TIMP-3 inhibitor and pentosidine AGEs were elevated with levels of active MMPs 2&9 were significantly reduced in BrM from AMD donors compared to age-matched controls (Kamei and Hollyfield, 1999; Ishibashi et al., 1998; Hammes et al., 1999; Hussain et al., 2011). Diminished metabolic support may therefore be the initial insult that progresses to the death of RPE and photoreceptors recruiting additional inflammatory responses or choroidal neo-vascularization (CNV).

Stimulation of the MMP pathway could therefore constitute a viable therapeutic option for eyes with precursor stages of AMD. As such, Ahir et al., 2002 demonstrated increased hydraulic conduc-tivity of aged BrM after cultivation with activated MMP 2 and MMP 9 isolated from cultured human RPE cells. These authors also showed that proliferating RPE cells release copious amounts of activated MMPs. It can thus be hypothesized that the resolution of drusen after conventional laser (Ho et al., 1999) or diode laser (Rodanant et al., 2002) treatment of RPE observed in clinical trials was caused by secretion of ECM-degrading enzymes by migrating and proliferating RPE cells during closure of the laser wound. However, both conventional continuous wave lasers (Roider et al., 1993a) and low energy diode lasers (Mojana et al., 2011), although targeting RPE, also cause irreversible collateral thermal damage to the outer retina. Therefore, in the clinical trials, laser treatment was applied only once, the number of laser spots was kept to a minimum and spots were delivered into the peripheral macula to avoid undue damage of the central macula (Ho et al., 1999; Rodanant et al., 2002; Owens et al., 2006; Maguire et al., 2006). Hence, improvement of visual function may be expected to be limited (Ho et al., 1999; Friberg et al., 2009) or absent (Owens et al., 2006).

Selective Retina Therapy (SRT) is a micropulse laser technique that selectively targets the RPE but spares the neurosensory retina without causing microscotoma (Brinkmann et al., 2006; Roider et al., 2000, 1999, 1993b, 1992). Selective damage of the RPE is achieved by formation and rapid expansion of microbubbles around the melanosomes in the RPE cells leading to disruption of the cell structure without thermal transients spreading into the adjacent tissue (Brinkmann et al., 2000). This confinement of heat flow to the interior of a given RPE cell ensures that the overlying photoreceptors and the underlying BrM with the choroid are spared from damage. The mechanism of SRT could enable the positive features of previous treatments for early AMD with conventional lasers to be harnessed without entertaining the negative effects such as the promotion of CNV or microscotoma in the central visual field.

The present investigation was designed to assess the potential use of the SRT technique for inducing the release of activated MMPs from RPE cells as a vehicle to address the pathological alterations of BrM associated with AMD. An explant culture system was initiated to allow the determination of RPE apical and basal compartment MMP release patterns and to assess the effect of the SRT laser using energy levels below and above the threshold of RPE cell disruption.

2. Materials and methods

2.1. Porcine RPE-choroid preparation

Fresh porcine eyes were obtained from a local abattoir and experiments were initiated within 3–4 h of death. Whole globes were briefly immersed in antiseptic solution. A circumferential incision at the pars plana allowed the removal of the anterior segment and vitreous followed by gentle peeling of the retina. The remaining globe was cut into quadrants and the RPE-BrM-choroid layer gently separated from the sclera using forceps and scissors. A suitably sized RPE-choroid preparation was then fixed between the two parts of a customized polyacetal fixation ring (modified part no. 1300, Minucells and Minutissue, Bad Abbach, Germany) with an exposed tissue diameter of 6 mm, Fig. 1a–c. Tissue mounted rings were then transferred to multiwell culture plates (Corning Costar, Lowell, MA, USA) and allowed to equilibrate for 6 h in culture medium. The culture medium was a mixture of equal amounts of Dulbecco's modified Eagle's medium (with glucose 4.5 g/l) (DMEM; PAA, Cölbe, Germany) and Ham-F12 medium (PAA) which was supplemented with penicillin/streptomycin (1%), L-glutamine, HEPES (10 mM), sodium pyruvate (110 mg/ml) and porcine serum (10%, PAA), taurine (100 μM), and calcium (2 mM).

2.2. Threshold laser energy for RPE cell death

The selective retina therapy (SRT) laser was a prototype Q-switched frequency doubled Nd:YLF laser with 527 nm wave-length, 200 μm spot diameter, 1.7 μs of pulse duration, 100 Hz of repetition rate, and with 30 pulses per irradiation being delivered via a slit lamp.

For the laser procedure the 12-well culture plates containing the RPE-choroid tissue rings (immersed in phenol red-free culture medium) were placed on the chin-rest and the laser beam was directed onto the RPE with a mirror attached to the slit lamp. Laser energies between 80 and 180 mJ/cm^2 were applied to 3 to 5 tissue preparations. Altogether, 90–100 spots were evenly distributed on the exposed RPE with a distance of one to two spot diameters between the spots. Following SRT, threshold energy for RPE cell death was determined by standard calcein-AM viability testing early (1 h) after SRT and after 24 h incubation in culture medium as previously described (Bussolati et al., 1995; Miura et al., 2010; Palma et al., 2008). Briefly, RPE-choroid preparations were incu-bated with calcein-AM (10 μg/ml, AnaSpec, San Jose, CA, USA) for 30 min and washed with PBS. Digital images were obtained with a fluorescence microscope (Zeiss, Jena, Germany) with
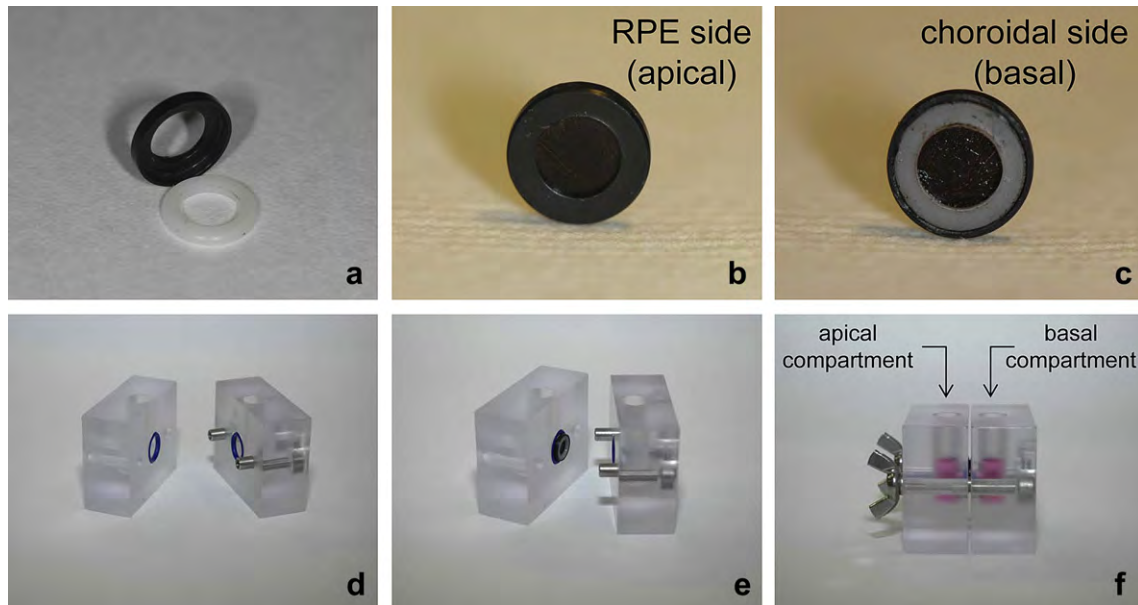
Fig. 1. Principle of the modified Ussing chamber. The RPE-choroid tissue preparation is clamped between the black and white fixation rings (a–c). The tissue ring is placed between the two halves of a modified Ussing chamber and thereby separates the two chamber compartments (d,e). The two compartments, referred to as "apical" (RPE-facing) and "basal" (choroid facing), are each filled with 1 ml culture medium (f).

$\lambda ex/\lambda em = 497/517$ nm and the fraction of dead cells within the area of the laser spot was determined using ImageJ (NIH, vers. 1.45e).

2.3. RPE wound healing after SRT

The RPE wound-healing response following SRT was characterized at various time points of incubation by calcein-AM staining as this method can be used to assess cell morphology and morphological evidence of apoptotic changes such as chromatin condensation and segregation in blebs, together with functional information about plasma membrane integrity (Bussolati et al., 1995; Palma et al., 2008). Tissue samples were retrieved from the Ussing chambers at days 1, 2, 4, and 6 after SRT and stained with calcein-AM as described above.

2.4. Vectorial release of MMPs from the RPE-choroid preparation

Mounting of the tissue-containing rings into a modified Ussing chamber (Fig. 1d–f) allowed the separation of apical (RPE-facing) and basal (choroid facing) half-compartments. This separation was mediated by the use of silicone rings on either side of the tissue-containing ring. Leak-tightness of the preparation was assessed in preliminary experiments after three days of culture in the Ussing chamber. Briefly, a vital stain (Brilliant blue G, Brilliant peel®, Fluoron, Ulm, Germany) was introduced into one half-compartment and its entry (if any) into the opposing half-compartment was monitored by measuring the absorbance at 584 nm (Thermo Fisher Scientific, Waltham, MA, USA). Cross-over of the stain was not observed in any of the preparations tested (data not shown).

Both control and irradiated (100, 140, and 180 mJ/cm^2; 80–90 200 μm spots per preparation) tissue rings were mounted into the Ussing chamber assembly and each half-compartment filled with 1 ml culture medium (see above) containing 1% porcine serum. Incubations were carried out in a humidified incubator at 37 °C with a gas mixture of 5% CO_2. Every 24 h the conditioned medium (from both half-chambers) was collected and replaced by fresh medium. The collected medium was centrifuged to remove cellular debris and the supernatant was stored at −20 °C until analysis of MMPs by zymography. At day 5 or 6 after SRT, the tissue ring was removed from the Ussing chamber and calcein-AM staining of the tissue was performed to confirm cell viability. Only medium samples obtained from tissue preparations with ≥90% vital cells were analysed for MMP content.

2.5. Zymography of released MMPs

Medium samples were obtained from both apical and basal half-compartments covering an incubation period of 1–6 days. Both control and SRT treated preparations were utilised. At the end of some experiments, a 5 mm trephine of the RPE-choroid preparation was also obtained to assess the MMP content within the tissue. This was mixed with 40 μl non-reducing zymogram sample buffer (Bio-Rad, Hercules, CA, USA), vortexed, spun and a 30 μl aliquot of the supernatant applied to gels. Also included on each gel was a 10 μl aliquot of incubation medium (containing 1% porcine serum) and molecular weight standards (Bio-Rad) to identify the gelatinases by their respective molecular weights. Additionally, to clearly identify latent and active forms of MMPs 2 and 9, activation of the gelatinases by amino-phenyl mercuric acetate (APMA, Sigma–Aldrich, Munich, Germany) was performed in preliminary experiments (data not shown).

For zymography 10 μl conditioned medium sample was mixed with 20 μl non-reducing zymogram sample buffer and the mixture loaded onto a 0.1% gelatin containing 10% SDS-PAGE gel (10% Ready Gel, Bio-Rad, USA). After electrophoresis (150 V, 1 h), gels were incubated for two half-hour periods in renaturation buffer (Bio-Rad). Gels were then transferred to development buffer (Bio-Rad) and incubated at 37 °C for 16 h to allow proteolytic digestion of the gelatine substrate. In accordance with other reports, we chose an incubation period of 16 h which has been found optimal with 10% SDS-PAGE gels to obtain good separation of all MMP species in ocular tissues (Ahir et al., 2002; Hussain et al., 2010a, 2011) and certain non-ocular tissues (Kim et al., 2011; Lee et al., 2010; Zhou et al., 2011. Indeed, our experiments with prolonged incubation of 42 h compared to 16 h incubation showed no additional bands. On

the contrary, longer incubations risked masking the presence of minor bands that normally ran in close proximity to the major bands. Gels were stained with Commassie blue (Bio-Rad) for a period of 3 h. De-staining was carried out with de-staining solution (Bio-Rad) for about 1.5 h. MMP activity was observed as clear bands on a blue background. Digital images of the gels were obtained with a CCD camera in a chemiluminescence system (Biostep, Jena, Germany).

For quantification of the MMP activity, the gelatinase bands were analysed with 1D gel analysis software (TotalLab TL100, TotalLab Ltd., Newcastle, UK). Each gel contained 2–3 samples of untreated controls and every set of experiment was performed 5–10 times. The MMP activity of the laser-treated samples was calculated as fold of the mean of the controls.

2.6. Histology

For light microscopy the RPE-choroid preparations were fixed in 4% formaldehyde, dehydrated in a graded series of ethanol and embedded in paraffin. Three μm sections were stained with hematoxylin-eosin and examined with light microscopy. Digital images were obtained with the AxioCamMRc5 (Zeiss, Jena, Germany).

2.7. Statistical analysis

Statistical analyses were performed using the unpaired Student's t-test. Values reported in figures represent mean ± standard error of the mean (SEM). The level of significance for all tests was $p < 0.05$.

3. Results

3.1. RPE-choroid organ culture

Calcein-AM staining confirmed the structural integrity of the monolayer with preservation of morphological characteristics of the RPE cells over an examined incubation period of 6–7 days (Fig. 2a,b). Cell viability remained intact over this period under restricted nutritional conditions with 1% porcine serum supplement in the medium. Paraffin embedded cross-sections of three RPE-choroid preparations showed polarized RPE cells with basal nuclei and apical pigment granules after 24 h of incubation (Fig. 2c). At day 6 of incubation, the great majority of RPE cells remained polarized while some RPE cells began to flatten (Fig. 2d).

3.2. RPE threshold of cell death and wound healing after SRT

Calcein-AM cell viability staining was performed early (1 h) after SRT and following 24 h incubation period after SRT. Rather than a clearly defined threshold of cell death, we found a transition zone (Table 1). All exposed cells survived laser energies of 80 and 100 mJ/cm^2. 120 and 140 mJ/cm^2 did not result in early cell death but calcein staining 24 h after laser revealed 30–50% dead RPE cells within the irradiated area after 120 mJ/cm^2 and 50–100% dead RPE cells after 140 mJ/cm^2 depending on cell pigmentation. 160 mJ/cm^2 led to early cell death of 30–50% of exposed cells assessed 1 h following SRT. Laser energies of 180 mJ/cm^2 resulted in early cell death of 50–100% RPE cells within the laser spot (Fig. 3a). 160 and 180 mJ/cm^2 lead to cell death of all exposed cells 24 h after SRT. Two days after SRT, RPE cells at the edge of the laser spot began to stretch and migrated towards the centre of the wound and the nucleus became visible (Fig. 3b). At day 4 after SRT, enlarged RPE cells almost covered the wound with prominent nuclear staining in these cells (Fig. 3c). At day 6 after SRT, irregularly shaped RPE cells

grew confluent and covered the wound. The nucleus was still prominent. Some RPE cells within the spot had two nuclei (Fig. 3d).

3.3. MMP release profiles of untreated RPE-choroid preparations (control)

A representative zymogram showing the differential release patterns of MMPs into the apical (RPE-facing) and basal (choroid facing) compartments of the Ussing chamber (at day 3 of incubation) together with the MMP species present in the tissue extract (at day 5, i.e., at termination of experiment) is given in Fig. 4a.

3.3.1. Apical compartment
Pro-MMP 9 (98 kDa) was always found in the culture medium of the apical compartment. In contrast, only small amounts of active MMP 9 (88 kDa) were sporadically detected. We found two forms of pro-MMP 2 (isoform 1 (65 kDa) and isoform 2 (62 kDa)) in the apical compartment. Active MMP 2 (56 kDa) was not detected in the apical compartment (or if present, was below our detection limit).

3.3.2. Basal compartment
As in the apical compartment, pro-MMP 9 was always found in the culture medium of the basal compartment and only small amounts of active MMP 9 were sporadically detected. Again, the two forms of pro-MMP 2 (isoform 1 and isoform 2) were also found. In contrast to the apical compartment, active MMP2 was consistently present in the basal compartment from day 2 of the incubation period.

3.3.3. RPE-choroid tissue extract
As in the apical and basal compartments, pro-MMP 9 was always found in the tissue extract whereas only small amounts of active MMP 9 were detected. Two forms of pro-MMP 2 (isoform 1 and isoform 2) and, again in contrast to the apical compartment, the active form of MMP 2 was found to be present in the tissue extract.

3.4. MMP release profiles of RPE-choroid preparations after SRT

A representative zymogram of the MMP changes in the various compartments of the RPE-choroid preparation after SRT is shown in Fig. 4b. Levels of pro-MMP 2 were elevated in all compartments. Active MMP 2 was elevated in the basal compartment and the tissue fraction. Pro-MMP 9 levels were not altered. Time course of changes in MMPs are given in detail below for individual compartments (Figs. 5–7).

MMP profile in detail:

3.4.1. Apical compartment
Levels of pro-MMP 9 were not significantly altered after SRT at all three energy levels tested (Fig. 5a). SRT with 180 mJ/cm^2 increased pro-MMP 2 isoform 1 up to 1.5 fold (SEM ± 0.1, $p < 0.05$), and pro-MMP 2 isoform 2 up to 1.6 fold (SEM ± 0.1, $p < 0.05$) at day 3 after laser. SRT with 140 mJ/cm^2 increased isoform 1 up to 1.9 fold (SEM ± 0.4, $p < 0.05$) and isoform 2 up to 1.7 fold (SEM ± 0.2, $p < 0.05$) at day 4 after irradiation. Laser energy of 100 mJ/cm^2 was without effect on levels of pro-MMP 2 (Fig. 5b,c). Elevations in the levels of pro-MMP 2 had returned to baseline values by days 5–6 after SRT. Active MMP 2 was not detected in the apical compartment.

3.4.2. Basal compartment
The release of pro-MMP 9 was not influenced by SRT at any of the energy levels utilised (Fig. 6a). SRT with 180 mJ/cm^2 increased pro-MMP 2 isoform 1 2.1 fold (SEM ± 0.4, $p < 0.05$) and pro-MMP 2
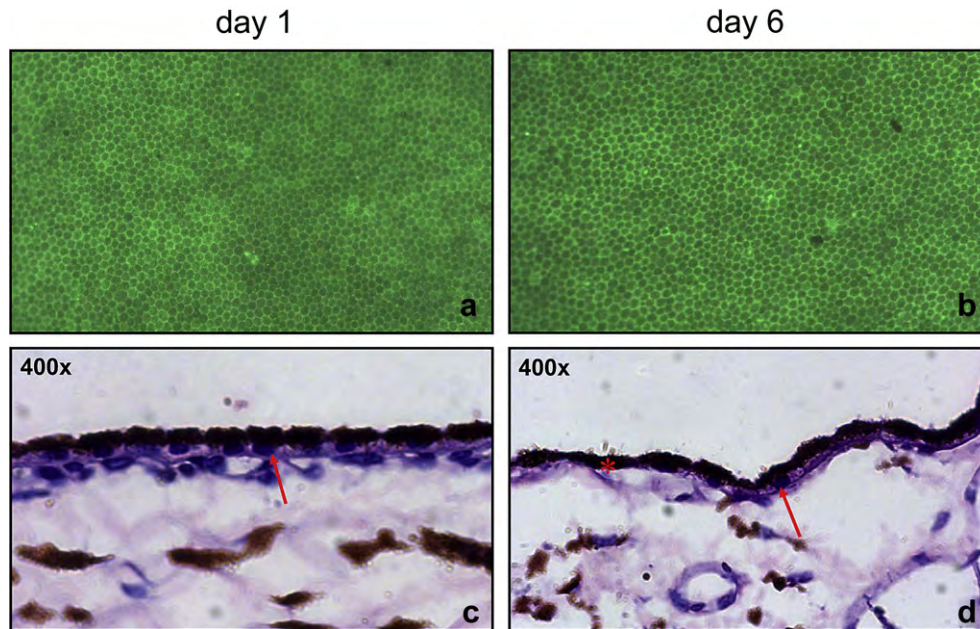
Fig. 2. RPE cell viability and morphology. Cell viability test (Calcein staining) at day 1 of cultivation (a) and day 6 (b) confirms cell viability and well preserved cell morphology (green = vital cells, black spots = dead cells). c,d: Paraffin embedded cross-sections (HE staining, original magnification 400×). After 24 h of cultivation the rectangular RPE cells are well polarized with basal nuclei and apical pigment (arrow) (c). After 6 days most cells remain polarized (arrow) while few cells appear flattened (*) (d). (For interpretation of the references to colour in this figure legend, the reader is referred to the web version of this article.)

isoform 2 1.6 fold (SEM $\pm$ 0.2, $p < 0.05$) three days after laser treatment. SRT with 140 mJ/cm^2 increased isoform 1 1.9 fold (SEM $\pm$ 0.4, $p < 0.05$) and isoform 2 1.5 fold (SEM $\pm$ 0.07, $p < 0.05$) at this same time period (Fig. 6b,c). Levels of active MMP 2 were very low and difficult to quantify at day 1 in both control and laser-treated samples. Thereafter, levels were increased allowing a comparative assessment. In contrast to the RPE-facing compartment, the active form of MMP 2 was found in the basal compartment from day 2 of cultivation until the end of the incubation period (Fig. 6d). SRT with 180 mJ/cm^2 increased its release 1.5 fold (SEM $\pm$ 0.1, $p < 0.05$) at day 2 and 1.6 fold (SEM $\pm$ 0.2, $p < 0.05$) at day 3. SRT with 140 mJ/cm^2 increased its release 1.4 fold at day 2 and 3 but this was statistically not significant (SEM $\pm$ 0.2, $p = 0.06$). Exposure to laser energy with 100 mJ/cm^2 did not alter the release of active MMP 2.

3.4.3. RPE-choroid tissue extract (5 days after SRT)

The level of pro-MMP 9 in the tissue extract was not significantly altered after SRT (Fig. 7a). The active form of MMP 9 was found in some samples but at variable degrees and with low reproducibility (data not shown). The pro-forms of MMP 2 increased 1.6 fold (SEM $\pm$ 0.3, $p < 0.05$, isoform 1) and 1.65 fold (SEM $\pm$ 0.1, $p < 0.05$, isoform 2) after 180 mJ/cm^2. After SRT with 140 mJ/cm^2 the expression isoform 1 increased 1.5 fold (SEM $\pm$ 0.1, $p < 0.05$) without significant changes in isoform 2 (Fig. 7b). The active form of MMP 2 increased 1.9 fold (SEM $\pm$ 0.2, $p < 0.05$) after SRT with 180 mJ/cm^2 with lower energy levels being without effect

(Fig. 7c). Exposure to laser energy of 100 mJ/cm^2 did not alter the level of any of the gelatinase species.

4. Discussion

As opposed to previously used organ culture (Del Priore et al., 1989; Flaxel et al., 2007; Miura et al., 2010) and cell culture models (Ahir et al., 2002), the newly established modified Ussing-chamber system of the present study has allowed an assessment of the differential release profile of MMPs from the apical and basal aspects of an intact RPE monolayer. In both control and lasered preparations, the release of pro-MMPs 2&9 occurred primarily into the basal compartment. Furthermore, very little of these latent enzymes were actually retained in the tissue compartments (Fig. 4). Several studies have demonstrated the release of MMPs 2&9 from RPE cells but in our RPE-choroid preparation, the possibility of contribution from choroidal endothelial cells should also be considered (Ahir et al., 2002; Hollborn et al., 2007; Irschick et al., 2009). This contribution is likely to be minimal (if any) as incubation of isolated human Bruch's-choroid preparations was not associated with the release of any detectable amounts of MMPs (Ahir et al., 2002).

Presence of serum is essential for the release of MMPs. In its absence, MMPs are synthesised by the RPE but retained within the cells (Ahir et al., 2002). For in-vitro work therefore, sufficient amounts of serum must be included in the incubation mixture to ensure MMP release but levels should not be so high as to mask the endogenous release of these enzymes. The present study utilised 1% porcine serum and this was high enough to ensure release of MMPs and yet low enough to allow the detection of small amounts of MMPs released in the apical compartment (Fig. 4a).

SRT at energy levels of 140 and 180 mJ/cm^2 resulted in the transient increase in levels of pro-MMP 2 in both half-compartments and an increase in active MMP 2 in the basal compartment. This increase was not the result of release from laser-damaged cells since levels of pro-MMP 9 were not altered.

Table 1
Threshold laser energies for RPE cell death.

Time after SRT	SRT laser energy (mJ/cm^2)					
	180	160	140	120	100	80
1 h	50–100%	30–50%	0%	0%	0%	0%
24 h	100%	100%	50–100%	30–50%	0%	0%

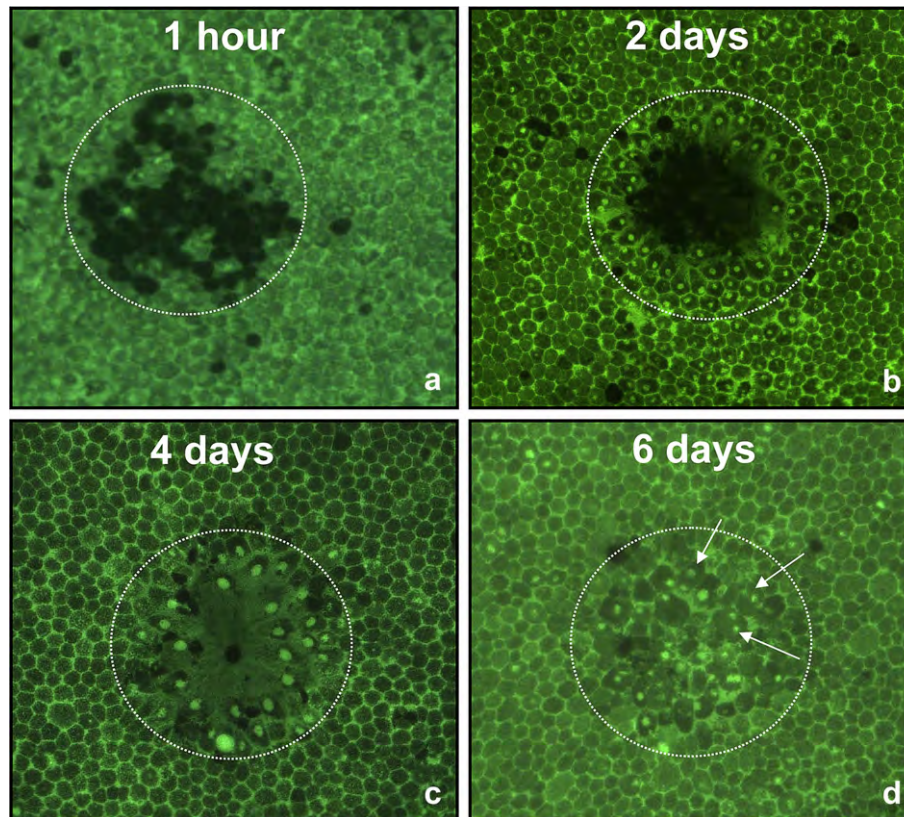Percentage of dead cells within the laser spot 1 h and 24 h after SRT.

Fig. 3. RPE wound healing after SRT. a: One hour after SRT with 180 mJ/cm^2 calcein staining showed that 50% of the exposed RPE cells were dead (black spots). b: Two days after SRT the RPE cells at the edge of the laser spot began to stretch towards the centre of the wound. c: At day 4 after SRT large RPE cells covered the wound. Calcein showed prominent nucleus staining in these cells d: At day 6 after SRT irregularly shaped RPE cells grew confluent and covered the wound. The presence of two nuclei in some RPE cells within the spot suggests mitosis and cell proliferation during wound healing (arrows).

Also the observed increase in MMP 2 occurred with a delay of 2 days after SRT and for up to 6 days despite the fact that the medium was changed every 24 h. The time course of release of pro-MMP 2 after laser in the apical compartment was much broader than changes in the basal compartment. These differential effects on either side of the RPE monolayer and the detection of active MMP 2 only in the basal compartment may be related to the micro-environment on opposite sides of the in-vitro preparation. Released MMPs from the apical surface of the RPE would rapidly enter the bulk solution and therefore there is no delay in release and appearance of MMPs in the sampled solution. In the case of pro-MMP 2, this rapid dilution together with fact that lower levels are released means that the concentration may not be sufficient for effective binding to the membrane bound MMP14–TIMP2 complex and subsequent activation (Strongin et al., 1995; Butler et al., 1998). On the other hand, release at the basal aspect of the RPE cells means that the MMP molecules must traverse BrM and the choroidal mass before they enter the bulk solution in the half-compartment of the Ussing chamber. This transit route could be associated with binding to the matrix and sequestration into high molecular weight complexes and may be the reason for the short period that their levels are elevated in the basal compartment (Kumar et al., 2010; Hussain et al., 2010a). Similarly, the higher level of basolateral release of pro-MMP 2 together with transitory confinement between the RPE and BrM allows greater likelihood of interaction with the MMP14–TIMP2 complex leading to the release of activated MMP 2.

A secondary aim of this study was to determine whether sub-threshold laser energy (that is, laser energy just below the threshold of RPE cell disruption) would suffice to increase the expression of MMP as a sub-lethal shock reaction. Our results clearly show that a transient increase of basal MMP expression and release can only be triggered by detachment and migration of RPE cells during wound re-surfacing. Hence, in order to trigger increased release of MMP, RPE cells must be destroyed or removed so that neighbouring cells can migrate. The determined threshold of cell disruption in this study was in accordance with earlier results (Brinkmann et al., 2000). Prominent nuclear staining and the presence of two nuclei in some RPE cells within the spot (Fig. 3c,d) indicate RPE proliferation as RPE migration and proliferation after localized mechanical (Hergott and Kalnins, 1991; Kiilgaard et al., 2007) or laser (Flaxel et al., 2007; von Leithner et al., 2010) injury of an intact RPE cell layer has been demonstrated by several other investigators.

Although proliferating RPE cells in culture have been shown to release active MMPs 2&9 in a cell cycle dependent manner (Ahir et al., 2002), in the present study, using a 200 μm spot size, only increases in pro- and active MMP 2 were apparent with no change in levels of pro- or active MMP 9. A previous study, using conventional lasers with a 200 μm spot size and human RPE explants demonstrated increased production of pro-MMP 2 but failed to report on changes in active MMP 2. These authors were also unable to detect the presence of pro- or active MMP 9 in their preparations (Flaxel et al., 2007). The discrepancy in the release of active MMP 9 between cell culture and laser studies may lie in the size of the laser spots utilised. With a 200 μm spot, both this study and that of Flaxel et al. (2007) showed the wound to be resurfaced with RPE cells within 4–6 days after the lesion. This short time would suggest that
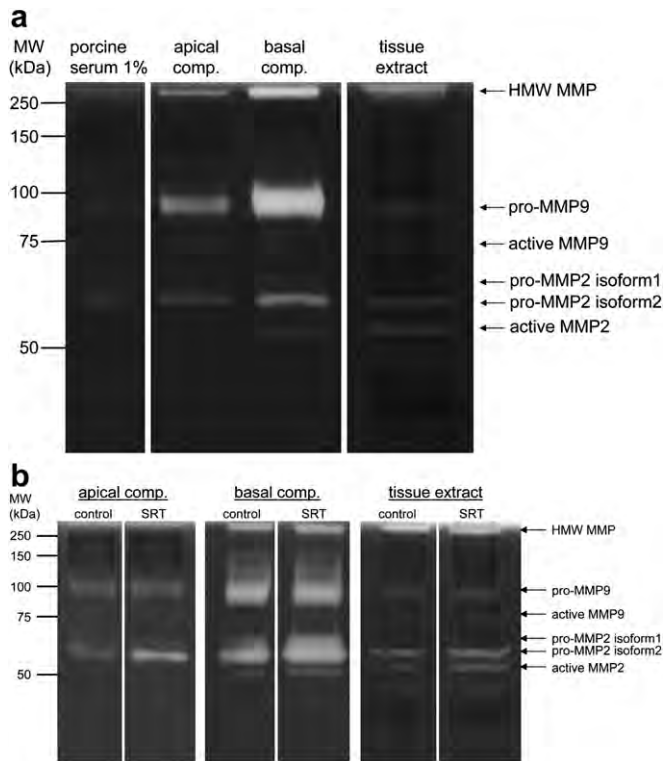
Fig. 4. a: Polarized release and expression of MMP without SRT. Representative zymogram of MMP 2 and 9 species in conditioned culture medium of the apical and basal compartment of the Ussing chamber (at day 3) and in the tissue extract (vortexed RPE-Bruch's membrane-choroid at day 5). Pro-MMP 9 (98 kDa) was found in the apical and basal compartment and in the tissue extract. Active MMP 9 (88 kDa) was only sporadically detectable. Two forms of pro-MMP 2 (isoform 1 (65 kDa) and isoform 2 (62 kDa)) were found in the apical and basal compartment and in the tissue extract. Active MMP 2 (56 kDa) was not found in the medium of the apical compartment but in the medium of the basal compartment and in the tissue extract. Lane 1: background MMP activity in 1% porcine serum. HMW = High molecular weight complexes of MMP 2 and 9. b: Increase of MMP 2 after SRT. Representative zymograms showing the increase of MMP 2 at day 3 (apical and basal compartment) and day 5 (tissue extract) after SRT with energy levels above threshold for RPE cell death. The active form of MMP 2 is only found in the basal compartment and in the tissue extract. MMP 9 did not increase after SRT. HMW = High molecular weight complexes of MMP 2 and 9.

Fig. 5. MMP profile (apical compartment) after SRT. Activity of pro-MMP 2 and 9 in the conditioned medium of the apical compartment after SRT with different laser energies. Activity is shown as fold of untreated controls (mean ± SEM). Pro-MMP 9 (a) is not influenced by SRT. Pro-MMP 2 (isoform1) significantly increases 2–4 days after SRT with 140 mJ/cm² and 2–3 days after SRT with 180 mJ/cm². Isoform 2 significantly increases 2–5 days after SRT with 140 mJ/cm² and 2–4 days after SRT with 180 mJ/cm² (b,c). The active form of MMP 2 is not found in the apical compartment ($^*p < 0.05$).

relatively few cells were actually migrating and may be the reason for the lack of release of active MMP 9.

MMP 2 plays an important role in the normal regulation of an ECM (Alcazar et al., 2007; Marin-Castano et al., 2005, 2006). Impaired MMP 2 activity due to applied oxidative stress has been shown to increase the levels of collagen types I and IV and laminin, components that are substrates for MMP 2 and are involved in sub-RPE deposit formation and gradual thickening of BrM (Alcazar et al., 2007). In BrM, levels of active MMP 2 have been shown to be reduced in both normal ageing (Guo et al., 1999) and in AMD (Hussain et al., 2011). Therapeutic intervention that could elevate levels of active MMP 2 would therefore appear to be a logical step towards the development of a treatment regime. Incubation of human BrM with active MMP 2 & 9 increased its hydraulic conductivity with MMP 9 being far more potent than MMP 2. Especially in BrM obtained from older donors, MMP 9 resulted in a pronounced increase of hydraulic conductivity (Ahir et al., 2002). Clinically, induction of ECM-degrading activity to such an extent as experimentally shown for MMP 9 (Ahir et al., 2002) would be undesirable in a potential treatment designed to modulate ECM turnover of BrM because excessive expression of active MMP 9 may trigger the formation of CNV (Lambert et al., 2002, 2003). This
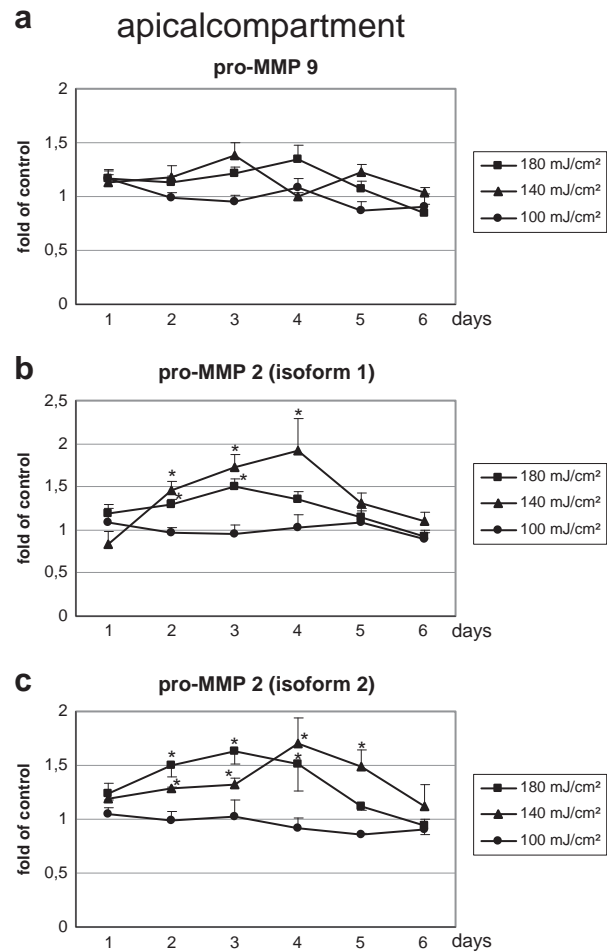
hypothesis is supported by the finding of positive feedback regulation between MMP 9 and vascular endothelial growth factor (VEGF), whereas MMP 2 down-regulated the VEGF expression of RPE cells (Hollborn et al., 2007). Experimental data by Amin et al. (2004) indicate that MMP 2 is constitutively expressed in the RPE whereas MMP 9 seems to be up-regulated under pathological conditions, e.g. in a chronic inflammatory milieu which is also suspected in eyes affected by AMD. As such, the expression of MMP 9 was increased while that of MMP 2 was decreased after stimulation of ARPE-19 cells with the pro-inflammatory cytokine TNF-alpha (Amin et al., 2004).

The SRT-induced moderate increase of active MMP 2 secretion on the basal side of the RPE (where the enzyme is in direct contact with BrM) but not on the apical side (where it could cause undue damage to the photoreceptors) together with un-altered levels of MMP 9 found in the present study points towards a potential of SRT as a treatment designed to slow macular ageing while avoiding the promotion of CNV. Ideally, laser intervention should be targeted as close to the fovea as possible. Since SRT spares photoreceptors, laser lesions can be delivered closer to the fovea in comparison to conventional lasers of previous studies (Ho et al., 1999; Owens et al., 2006). Others have used an 810-nm diode laser which was

a

basalcompartment
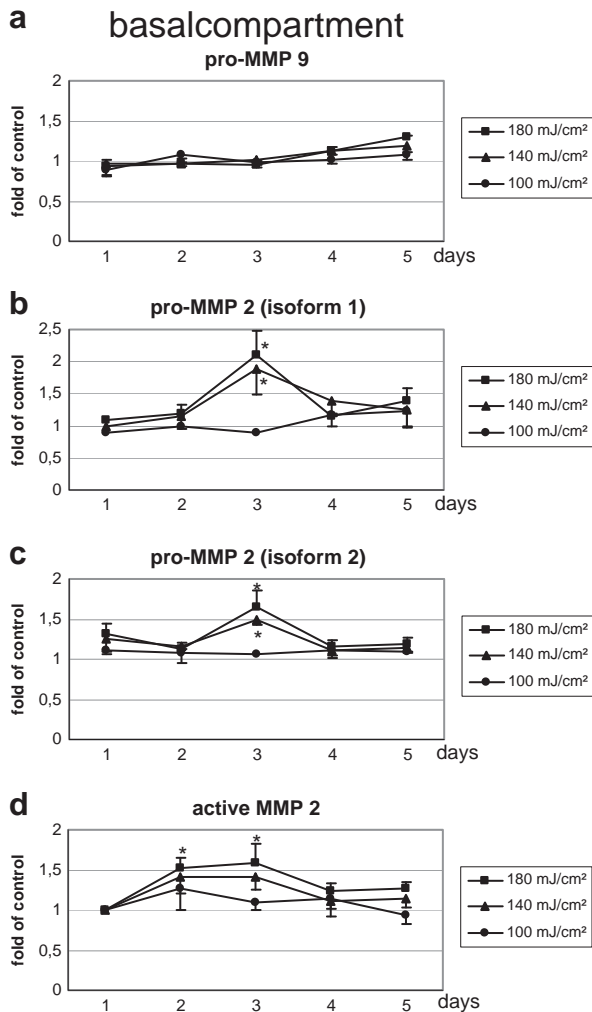

b

c

d

Fig. 6. MMP profile (basal compartment) after SRT. Activity of MMP 2 and 9 in the conditioned medium of the basal compartment after SRT with different laser energies. Activity is shown as fold of untreated controls (mean ± SEM). Pro-MMP 9 (a) is not influenced by SRT. Both isoforms of pro-MMP 2 increase with a significant peak 3 days after SRT with energy levels above the threshold for RPE cell death (140 and 180 mJ/cm^2) (b,c). Active MMP 2 is found from day 2 of cultivation and is significantly increased 2 and 3 days after SRT with 180 mJ/cm^2 (d) ($^*p < 0.05$).

claimed to produce "sub-threshold" lesions (Rodanant et al., 2002; Friberg et al., 2009). However, recent optical coherence tomography investigations have shown that photoreceptors are damaged by the laser (Mojana et al., 2011).

In clinical practice a desired therapeutic effect of SRT may be transient and therefore repeated treatments may become necessary and because SRT spares photoreceptors, it can be applied repeatedly. Repeated applications of SRT may not reduce the overall number of RPE cells because during RPE wound healing, besides migration of neighbouring cells, central and peripheral cells proliferate within 48 h (Kiilgaard et al., 2007; von Leithner et al., 2010).

In the present study, using porcine tissue, it was relatively straightforward to obtain a laser energy that just damaged RPE cells. In clinical practice, due to patient variation in fundus pigmentation, acoustic online dosimetry could be employed to apply the minimal laser energy to trigger the expression of MMP activity (Schuele et al., 2005).

Future laboratory work should be directed at the assessment of messenger RNA of MMPs in the RPE as well as an assessment of MMP inhibitors, angiogenetic, and pro-inflammatory growth factors following SRT.
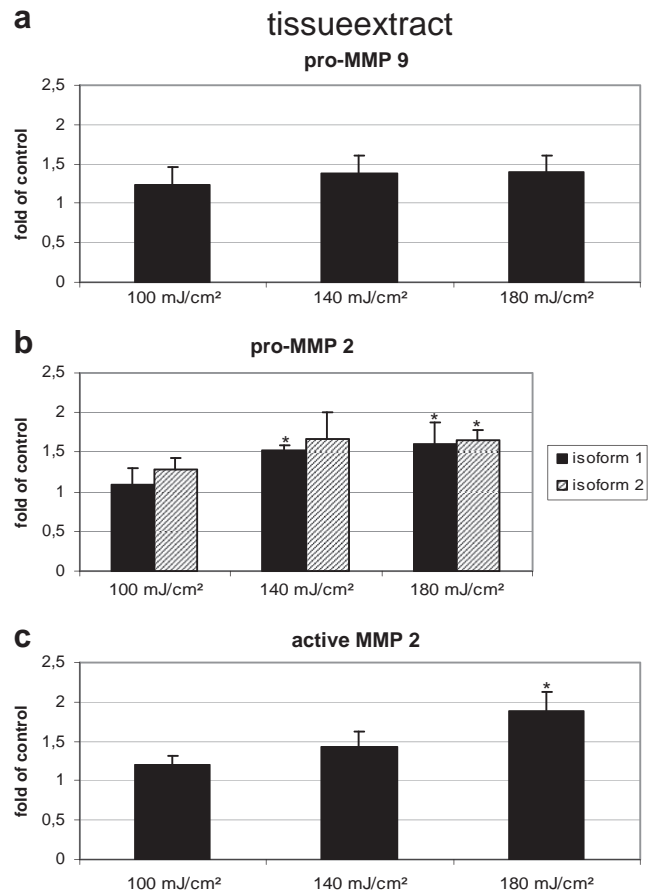
a

tissueextract

b

c

Fig. 7. MMP profile (tissue extract) after SRT. Activity of MMP 2 and 9 in the tissue extract at day 5 after SRT with different laser energy levels. Activity is shown as fold of untreated controls (mean ± SEM). The level of pro-MMP 9 was not altered by SRT (a). Both isoforms of pro-MMP 2 (b) and active MMP 2 (c) significantly increased after SRT with laser energy levels above threshold for RPE cell death (140 and 180 mJ/cm^2) ($^*p < 0.05$).

Conflict of interest

The work in this article has been carried out in accordance with the Uniform Requirements for Manuscripts submitted to Biomedical journals.

All authors disclose any actual or potential conflict of interest including any financial, personal or other relationships with other people or organizations within three years of beginning the submitted work that could inappropriately influence, or be perceived to influence, their work.

The work described has not been published previously and it is not under consideration for publication elsewhere, its publication is approved by all authors and tacitly or explicitly by the responsible authorities where the work was carried out, and if accepted, it will not be published elsewhere including electronically in the same form, in English or in any other language, without the written consent of the copyright-holder.

Each author has materially participated in the research and/or article preparation.

References

Ahir, A., Guo, L., Hussain, A.A., Marshall, J., 2002. Expression of metalloproteinases from human retinal pigment epithelial cells and their effects on the hydraulic conductivity of Bruch's membrane. Invest. Ophthalmol. Vis. Sci. 43, 458–465.

Alcazar, O., Cousins, S.W., Marin-Castano, M.E., 2007. MMP-14 and TIMP-2 over-expression protects against hydroquinone-induced oxidant injury in RPE:

implications for extracellular matrix turnover. Invest. Ophthalmol. Vis. 48, 5662–5670.

Alexander, J.P., Bradley, J.M., Gabourel, J.D., Acott, T.S., 1990. Expression of matrix metalloproteinases and inhibitor by human retinal pigment epithelium. Invest. Ophthalmol. Vis. 31, 2520–2528.

Amin, S., Chong, N.H., Bailey, T.A., Zhang, J., Knupp, C., Cheetham, M.E., Greenwood, J., Luthert, P.J., 2004. Modulation of Sub-RPE deposits in vitro: a potential model for age-related macular degeneration. Invest. Ophthalmol. Vis. Sci. 45, 1281–1288.

Brinkmann, R., Huttmann, G., Rogener, J., Roider, J., Birngruber, R., Lin, C.P., 2000. Origin of retinal pigment epithelium cell damage by pulsed laser irradiance in the nanosecond to microsecond time regimen. Lasers Surg. Med. 27, 451–464.

Brinkmann, R., Roider, J., Birngruber, R., 2006. Selective retina therapy (SRT): a review on methods, techniques, preclinical and first clinical results. Bull. Soc. Belge. Ophtalmol. 302, 51–69.

Bussolati, O., Belletti, S., Uggeri, J., Gatti, R., Orlandini, G., Dall'Asta, V., Gazzola, G.C., 1995. Characterization of apoptotic phenomena induced by treatment with L-asparaginase in NIH3T3 cells. Exp. Cell Res. 220, 283–291.

Butler, G.S., Butler, M.J., Atkinson, S.J., Will, H., Tamura, T., Schade van Westrum, S., Crabbe, T., Clements, J., d'Ortho, M.P., Murphy, G., 1998. The TIMP-2 membrane type I metalloproteinase 'receptor' regulates the concentration and efficient activation of progelatinase A: a kinetic study. J. Biol. Chem. 273, 871–880.

Del Priore, L.V., Glaser, B.M., Quigley, H.A., Green, W.R., 1989. Response of pig retinal pigment epithelium to laser photocoagulation in organ culture. Arch. Ophthalmol. 107, 119–122.

Della, N.G., Campochiaro, P.A., Zack, D.J., 1996. Localization of TIMP-3 mRNA expression to the retinal pigment epithelium. Invest. Ophthalmol. Vis. Sci. 37, 1921–1924.

Fariss, R.N., Apte, S.S., Olsen, B.R., Iwata, K., Milam, A.H., 1997. Tissue inhibitor of metalloproteinases-3 is a component of Bruch's membrane of the eye. Am. J. Pathol. 15, 323–328.

Flaxel, C., Bradle, J., Acott, T., Samples, J.R., 2007. Retinal pigment epithelium produces matrix metalloproteinases after laser treatment. Retina 27, 629–634.

Friberg, T.R., Brennen, P.M., Freeman, W.R., Musch, D.C., 2009. Prophylactic treatment of age-related macular degeneration report number 2: 810-nanometer laser to eyes with drusen: bilaterally eligible patients. Ophthalmic Surg. Lasers Imaging 40, 530–538.

Guo, L., Hussain, A.A., Limb, G.A., Marshall, J., 1999. Age-dependent variation in metalloproteinase activity of isolated human Bruch's membrane and choroid. Invest. Ophthalmol. Vis. Sci. 40, 2676–2682.

Hamlin, C.R., Kohn, R.R., 1971. Evidence for progressive, age-related structural changes in post-mature human collagen. Biochim. Biophys. Acta 236, 458–467.

Hammes, H.P., Hoerauf, H., Alt, A., Schleicher, E., Clausen, J.T., Bretzel, R.G., Laqua, H., 1999. N(epsilon)(carboxymethyl)lysin and the AGE receptor RAGE colocalize in age-related macular degeneration. Invest. Ophthalmol. Vis. Sci. 40, 1855–1859.

Handa, J.T., Verzijl, N., Matsunaga, H., Aotaki-Keen, A., Lutty, G.A., te Koppele, J.M., Miyata, T., Hjelmeland, L.M., 1999. Increase in the advanced glycation end product pentosidine in Bruch's membrane with age. Invest. Ophthalmol. Vis. Sci. 40, 775–779.

Hergott, G.J., Kalnins, V.I., 1991. Expression of proliferating cell nuclear antigen in migrating retinal pigment epithelial cells during wound healing in organ culture. Exp. Cell Res. 195, 307–314.

Hillenkamp, J., Hussain, A.A., Jackson, T.L., Cunningham, J.R., Marshall, J., 2004a. The influence of path length and matrix components on ageing characteristics of transport between the choroid and the outer retina. Invest. Ophthalmol. Vis. Sci. 45, 1493–1498.

Hillenkamp, J., Hussain, A.A., Jackson, T.L., Cunningham, J.R., Marshall, J., 2004b. Taurine uptake by human retinal pigment epithelium: implications for the transport of small solutes between the choroid and the outer retina. Invest. Ophthalmol. Vis. Sci. 45, 4529–4534.

Ho, A.C., Maguire, M.G., Yoken, J., Lee, M.S., Shin, D.S., Javornik, N.B., Fine, S.L., 1999. Laser-induced drusen reduction improves visual function at 1 year. Choroidal Neovascularization Prevention Trial Research Group. Ophthalmology 106, 1367–1373.

Hollborn, M., Stathopoulos, C., Steffen, A., Wiedemann, P., Kohen, L., Bringmann, A., 2007. Positive feedback regulation between MMP-9 and VEGF in human RPE cells. Invest. Ophthalmol. Vis. Sci. 48, 4360–4367.

Holz, F.G., Sheraidah, G., Pauleikhoff, D., Bird, A.C., 1994. Analysis of lipid deposits extracted from human macular and peripheral Bruch's membrane. Arch. Ophthalmol. 112, 402–406.

Hunt, R.C., Fox, A., al, P.V., Sigel, M.M., Kosnosky, W., Choudhury, P., Black, E.P., 1993. Cytokines cause cultured retinal pigment epithelial cells to secrete metalloproteinases and to contract collagen gels. Invest. Ophthalmol. Vis. Sci. 34, 3179–3186.

Hussain, A.A., Lee, Y., Marshall, J., 2010a. High molecular-weight gelatinase species of human Bruch's membrane: compositional analyses and age-related changes. Invest. Ophthalmol. Vis. Sci. 51, 2363–2371.

Hussain, A.A., Starita, C., Hodgetts, A., Marshall, J., 2010b. Macromolecular diffusion characteristics of ageing human Bruch's membrane: implications for age-related macular degeneration (AMD). Exp. Eye Res. 90, 703–710.

Hussain, A.A., Lee, Y., Zhang, J.J., Marshall, J., 2011. Disturbed matrix metalloproteinase (MMP) activity of Bruch's membrane in age-related macular degeneration (AMD). Invest. Ophthalmol. Vis. Sci. 52 (7), 4459–4466.

Irschick, E.U., Haas, G., Troger, J., Ueberall, F., Huemer, H.P., 2009. Involvement of protein kinase C in phagocytosis of human retinal pigment epithelial cells and induction of matrix metalloproteinase secretion. Int. Ophthalmol. 29, 333–341.

Ishibashi, T., Murata, T., Hangai, M., Nagai, R., Horiuchi, S., Lopez, P.F., Hinton, D.R., Ryan, S.J., 1998. Advanced glycation end products in age-related macular degeneration. Arch. Ophthalmol. 116 (12), 1629–1632.

Kamei, M., Hollyfield, J.G., 1999. TIMP-3 in Bruch's membrane: changes during aging and in age-related macular degeneration. Invest. Ophthalmol. Vis. Sci. 40 (10), 2367–2375.

Karwatowski, W.S., Jeffries, T.E., Duance, V.C., Albon, J., Bailey, A.J., Easty, D.L., 1995. Preparation of Bruch's membrane and analysis of the age-related changes in the structural collagens. Br. J. Ophthalmol. 79, 944–952.

Kiilgaard, J.F., Prause, J.U., Prause, M., Scherfig, E., Nissen, M.H., la Cour, M., 2007. Subretinal posterior pole injury induces selective proliferation of RPE cells in the periphery in in vivo studies in pigs. Invest. Ophthalmol. Vis. Sci. 48, 355–360.

Kim, C.H., Lee, J.H., Won, J.H., Cho, M.K., 2011. Mesenchymal stem cells improve wound healing in vivo via early activation of matrix metalloproteinase-9 and vascular endothelial growth factor. J. Korean Med. Sci. 26, 726–733.

Kumar, A., El Osta, A., Hussain, A.A., Marshall, J., 2010. Increased sequestration of matrix metalloproteinases in ageing human Bruch's membrane: implications for ECM turnover. Invest. Ophthalmol. Vis. Sci. 51, 2664–2670.

Lambert, V., Munaut, C., Jost, M., Noel, A., Werb, Z., Foidart, J.M., Racik, J.M., 2002. Matrix metalloproteinase-9 contributes to choroidal neovascularization. Am. J. Pathol. 161, 1247–1253.

Lambert, V., Wielockx, B., Munaut, C., Galopin, C., Jost, M., Itoh, T., Werb, Z., Baker, A., Libert, C., Krell, H.W., Foidart, J.M., Noël, A., Rakic, J.M., 2003. MMP-2 and MMP-9 synergize in promoting choroidal neovascularization. FASEB J. 17, 2290–2292.

Lee, J.Y., Kim, H.S., Oh, T.H., Yune, T.Y., 2010. Ethanol extract of Bupleurum falcatum improves functional recovery by inhibiting matrix metalloproteinases-2 and -9 activation and inflammation after spinal cord injury. Exp. Neurobiol. 19, 146–154.

Maguire, M.G., Ying, G.-S., Alexander, J., Browning, D.J., Peskin, E., Folk, J.C., Antoszyk, A.N., Grunwald, J.E., Klein, M.L., Lyon, A., McCannel, C.A., Stoltz, R.A., Trese, M., Fine, S.L., 2006. Laser treatment in patients with bilateral large drusen: the complications of age-related macular degeneration prevention trial. Ophthalmology 113, 1974–1986.

Marin-Castano, M.E., Csaky, K.G., Cousins, S.W., 2005. Nonlethal oxidant injury to human retinal pigment epithelium cells causes cell membrane blebbing but decreased MMP-2 activity. Invest. Ophthalmol. Vis. Sci. 46, 3331–3340.

Marin-Castano, M.E., Striker, G.E., Alcazar, O., Catanuto, P., Espinosa-Heidmann, D.G., Cousins, S.W., 2006. Repetitive nonlethal oxidant injury to retinal pigment epithelium decreased extracellular matrix turnover in vitro and induced sub-RPE deposits in vivo. Invest. Ophthalmol. Vis. Sci. 47, 4098–4112.

Miura, Y., Klettner, A., Noelle, B., Hasselbach, H., Roider, J., 2010. Change of morphological and functional characteristics of retinal pigment epithelium cells during cultivation of retinal pigment epithelium-choroid perfusion tissue culture. Ophthalmic Res. 43, 122–133.

Mojana, F., Brar, M., Cheng, L., Bartsch, D.U., Freeman, W.R., 2011. Long-term SD-OCT/SLO imaging of neuroretina and retinal pigment epithelium after subthreshold infrared laser treatment of drusen. Retina 31, 235–242.

Moore, D.J., Clover, G.M., 2001. The effect of age on the macromolecular permeability of human Bruch's membrane. Invest. Ophthalmol. Vis. Sci 42, 2970–2975.

Moore, D.J., Hussain, A.A., Marshall, J., 1995. Age-related variation in the hydraulic conductivity of Bruch's membrane. Invest. Ophthalmol. Vis. Sci. 36, 1290–1297.

Mott, J.D., Khalifah, R.G., Nagase, H., Shield, C.F., Hudson, J.K., Hudson, B.G., 1997. Nonenzymatic glycation of type IV collagen and matrix metalloproteinase susceptibility. Kidney Int. 52, 1302–1312.

Nagai, N., Klimava, A., Lee, W.H., Izumi-Nagai, K., Handa, J.T., 2009. CTGF is increased in basal deposits and regulates matrix production through the ERK (p42/p44mapk) MAPK and the p38 MAPK signaling pathways. Invest. Ophthalmol. Vis. Sci. 50, 1903–1910.

Okubo, A., Rosa Jr., R.H., Bunce, C.V., Alexander, R.A., Fan, J.T., Bird, A.C., Luthert, P.J., 1999. The relationships of age changes in retinal pigment epithelium and Bruch's membrane. Invest. Ophthalmol. Vis. Sci. 40, 443–449.

Owens, S.L., Bunce, C., Brannon, A.J., Xing, W., Chisholm, I.H., Gross, M., Guymer, R.H., Holz, F.G., Bird, A.C., 2006. Prophylactic laser treatment hastens choroidal neovascularization in unilateral age-related maculopathy: final results of the drusen laser study. Am. J. Ophthalmol. 141, 276–281.

Palma, P.F., Baggio, G.L., Spada, C., Silva, R.D., Ferreira, S.I., Treitinger, A., 2008. Evaluation of annexin V and Calcein-AM as markers of mononuclear cell apoptosis during human immunodeficiency virus infection. Braz. J. Infect. Dis. 12, 108–114.

Pauleikhoff, D., Zuels, S., Sheraidah, G.S., Marshall, J., Wessing, A., Bird, A.C., 1992. Correlation between biochemical composition and fluorescein binding of deposits in Bruch's membrane. Ophthalmology 99, 1548–1553.

Ramrattan, R.S., van der Schaft, T.L., Mooy, C.M., de Bruijn, W.C., Mulder, P.G., de Jong, P.T., 1994. Morphometric analysis of Bruch's membrane, the choriocapillaris, and the choroid in aging. Invest. Ophthalmol. Vis. Sci. 35, 2857–2864.

Rodanant, N., Friberg, T.R., Cheng, L., Aurora, A., Bartsch, D., Toyoguchi, M., Corbin, P.S., El-Bradey, M.H., Freeman, W.R., 2002. Predictors of drusen reduction after subthreshold infrared (810 nm) diode laser macular grid photocoagulation for nonexudative age-related macular degeneration. Am. J. Ophthalmol. 134, 577–585.

Roider, J., Michaud, N.A., Flotte, T.J., Birngruber, R., 1992. Response of the retinal pigment epithelium to selective photocoagulation. Arch. Ophthalmol. 110, 1786–1792.

Roider, J., Michaud, N., Flotte, T., Birngruber, R., 1993a. Histology of retinal lesions after continuous irradiation and selective micro-coagulation of the retinal pigment epithelium. Ophthalmologe 90, 274–278.

Roider, J., Hillenkamp, F., Flotte, T., Birngruber, R., 1993b. Microphotocoagulation: selective effects of repetitive short laser pulses. Proc. Natl. Acad. Sci. U S A 90, 8643–8647.

Roider, J., Brinkmann, R., Wirbelauer, C., Laqua, H., Birngruber, R., 1999. Retinal sparing by selective retinal pigment epithelial photocoagulation. Arch. Ophthalmol. 117, 1028–1034.

Roider, J., Brinkmann, R., Wirbelauer, C., Laqua, H., Birngruber, R., 2000. Subthreshold (retinal pigment epithelium) photocoagulation in macular diseases: a pilot study. Br. J. Ophthalmol. 84, 40–47.

Schuele, G., Elsner, H., Framme, C., Roider, J., Birngruber, R., Brinkmann, R., 2005. Optoacoustic real-time dosimetry for selective retina treatment. J. Biomed. Opt. 10, 064022.

Starita, C., Hussain, A.A., Pagliarini, S., Marshall, J., 1996. Hydrodynamics of ageing Bruch's membrane: implications for macular disease. Exp. Eye Res. 62, 565–572.

Strongin, A.Y., Collier, I., Bannikov, G., Marmer, B.L, Grant, G.A., Goldberg, G.I., 1995. Mechanism of cell surface activation of 72kDa type IV collagenase. Isolation of the activated form of the membrane metalloproteinase. J. Biol. Chem. 270, 5331–5338.

Vater, C.A., Harris Jr., E.D., Siegel, R.C., 1979. Native cross-links in collagen fibrils induce resistance to human synovial collagenase. Biochem. J. 181, 639–645.

von Leithner, P.L, Ciurtin, C., Jeffery, G., 2010. Microscopic mammalian retinal pigment epithelium lesions induce widespread proliferation with differences in magnitude between center and periphery. Mol. Vis. 16, 570–581.

Vranka, J.A., Johnson, E., Zhu, X., Shepardson, A., Alexander, J.P., Bradley, J.M., Wirtz, M.K., Weleber, R.G., Klein, M.L., Acott, T.S., 1997. Discrete expression and distribution pattern of TIMP-3 in the human retina and choroid. Curr. Eye Res. 16, 102–110.

Yamada, Y., Ishibashi, K., Bhutto, I.A., Tian, J., Lutty, G.A., Handa, J.T., 2006. The expression of advanced glycation endproduct receptors in rpe cells associated with basal deposits in human maculas. Exp. Eye Res. 82, 840–848.

Zhou, J., Zhang, J., Chao, J., 2011. Porphyromonas gingivalis promotes monocyte migration by activating MMP-9. J. Periodontal Res.. doi:10.1111/j.1600-0765.2011.01427.x [Epub ahead of print].